

Research Journal of Pharmaceutical, Biological and Chemical Sciences

Glaucoma Detection in Optical Coherence Tomography Images Using Undecimated Wavelet Transform.

Rajan A*, and Ramesh G P.

Department of Electronics and communication engineering, St.Peter's University, Tamilnadu, India.

ABSTRACT

The lack of vision that can't be cured is called blindness. Among the various causes of blindness, glaucoma is one of the leading irreversible blindness. In this study, the detection of glaucoma is achieved by designing an image classification system using Undecimated Wavelet Transform (UWT). UWT is an enhancement of Discrete Wavelet Transform (DWT) in order to avoid the shift invariance caused by DWT. The proposed system uses UWT coefficients as features for the diagnosis of glaucoma. Due to the high dimensionality nature of UWT coefficients, the discriminant UWT coefficients are selected by an independent evaluation criterion. The proposed system is tested by cross validation approach using Support Vector Machine (SVM) classifier. Experimental results show that the proposed glaucoma detection system has a classification accuracy of 92.18%.

Keywords: Glaucoma detection, optical coherence tomography images, wavelets, undecimated wavelet transform, support vector machine classifier.

**Corresponding author*

INTRODUCTION

The two most important imaging modalities used for glaucoma detection are fundus and OCT images. Cup to Disc Ratio (CDR) is the one of the features used for glaucoma detection. The CDR determination from OCT images by segmenting optic nerve head is discussed in [1-2]. The Retinal Vitreal (RV) and Retinal Choroid (RC) boundaries are computed using hybrid edge thresholding and markov model respectively. From the intersection of boundaries, CDR is computed. An approach for glaucoma diagnosis using Spectral domain OCT is described in [3]. The diagnosis of glaucoma is achieved by evaluating parameters from retinal nerve fibre layer and macular regions. A complete solution for the segmentation of optic nerve head using morphological operators is discussed in [4]. The usage of macular pathology for the diagnosis of glaucoma is described in [5].

The RV and RC boundary extraction by two techniques based on morphological and wavelet transform are discussed in [6]. After boundary detection, CDR is computed by the use lateral extent of the disc and cup. Also, cup depth and retinal thickness are used for the diagnosis. The authors in [6] use multi thresholding approach for the detection of RC and RV boundaries in [7]. To smooth these boundaries, Bezier curve fitting approach is used and then CDR is computed for glaucoma diagnosis.

However, the CDR determination is very difficult for diabetic patients due to the merger of disc and cup boundaries [6]. Also, the improper segmentation of disc and cup region leads to misclassification. Hence, several authors consider the glaucoma diagnosis system as image classification system using both fundus and OCT images. An OCT image classification system using Principal Component Analysis (PCA) is described in [8]. The dimensionality reduced features; Eigen vectors from PCA are used for the diagnosis using SVM classifier. An image classification system using fundus images using wavelet transform is described in [9]. From the wavelet sub-bands energy features are extracted and KNN classifier is used for classification. Based on approach in [9], glaucoma diagnosis system using OCT images is discussed in [10]. It uses wavelet coefficients as features for the classification with SVM classification. A comparative study of wavelet features for glaucoma diagnosis by KNN and SVM classifier is discussed in [11].

In this paper, an efficient image classification system using UWT is developed for early detection of glaucoma. The rest of the paper is as follows: Section 2 gives an explanation of methods and materials used in the proposed glaucoma detection system. Section 3 discusses the results obtained by the proposed system and the final section concludes the proposed glaucoma detection system.

METHODS AND MATERIALS

The proposed OCT image classification system for the diagnosis of glaucoma consists of three modules; preprocessing, where the given OCT images are pre-processed, feature extraction in which wavelet features are extracted and finally classification stage, where the OCT images are classified into either glaucomatous or non-glaucomatous images. A brief representation of the proposed system is shown in Fig.1.

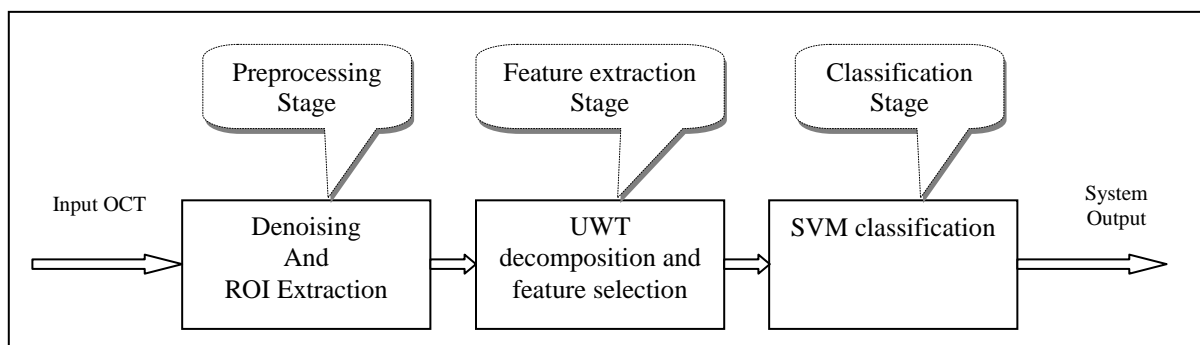


Fig 1: Proposed glaucoma diagnosis system using UWT and SVM

Preprocessing Stage

The first step in any pattern recognition or classification system is preprocessing. In this step, the noises in the OCT images are removed by applying median filtering of window size 7x7. Before de-noising, the colour space of the given OCT images is converted into gray scale in order to reduce the processing time and complexity of the system. Then, the de-noised images are further segmented using Otsu binary segmentation approach [12]. As the OCT images have two distinct regions; retinal area and background region, the Otsu segmentation works well. After segmentation, the retinal region is cropped and stored for further process after rescaled into a standard size of 64x128 pixels. Fig.2 shows the outputs of preprocessing stage.

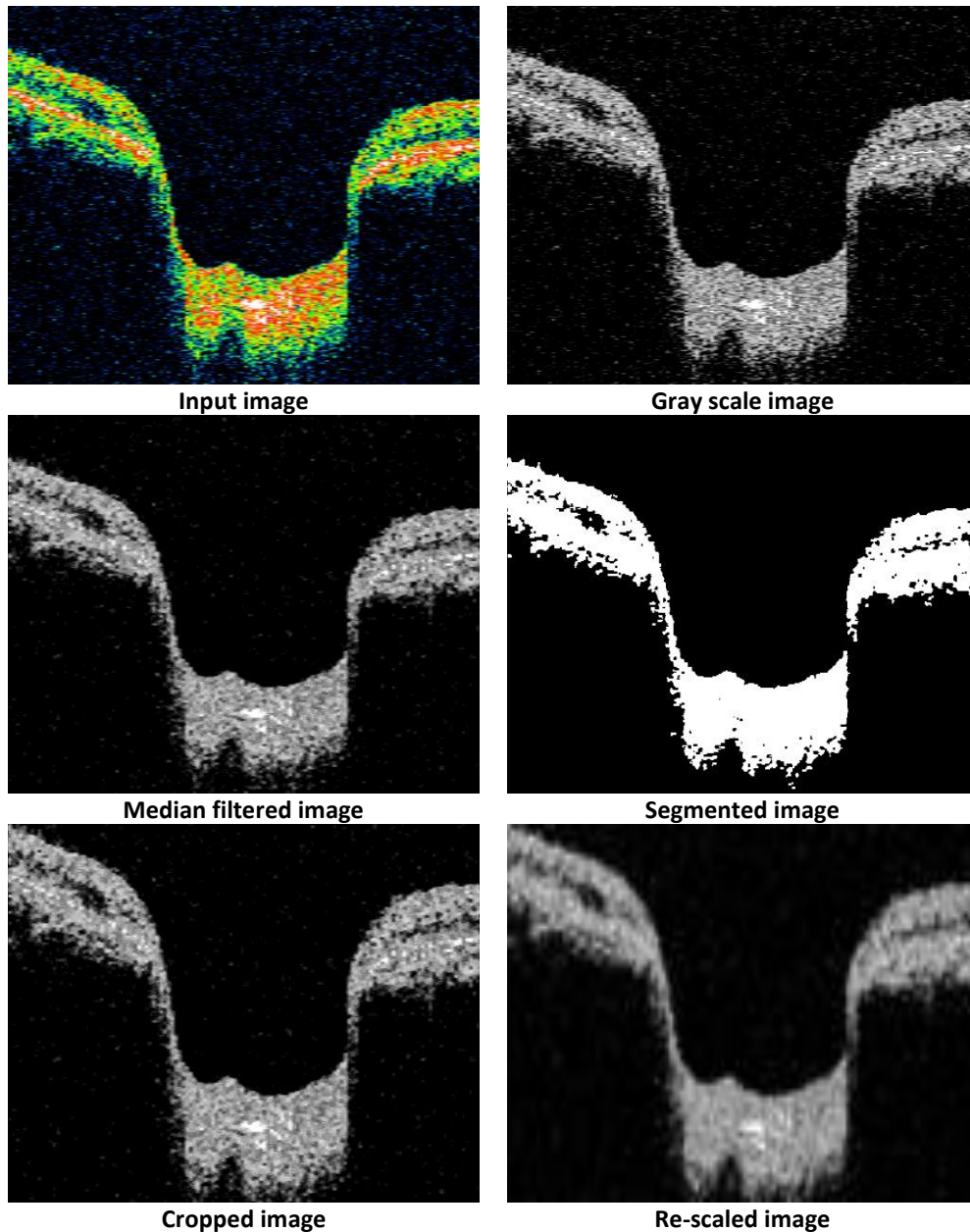


Fig 2: Simulation outputs - Preprocessing stage of the proposed glaucoma diagnosis system

Feature Extraction Stage

The input to the feature extraction stage is the pre-processed image obtained in the previous stage. This stage extracts the information in the form of feature vector for the classification of OCT images. Also, the

performance of a particular classification system depends on the features extracted in this stage. Fig.3 shows the extraction of features for the proposed glaucoma detection system.

The most widely used frequency domain transform in many image processing applications is wavelet transform [13]. In order to extract information for classification, the proposed system also uses wavelet transform. However, the main drawback of DWT is the lack of shift invariance which is caused by up and down-sampler in the design of wavelet filters. Hence, a small change in the input signal causes serious variations in the wavelet coefficients. To overcome this disadvantage of DWT, the design of DWT is modified by just removing the up and down-sampler which is called UWT. Fig. 4 (a) and (b) show the DWT and UWT decomposition filter design respectively.

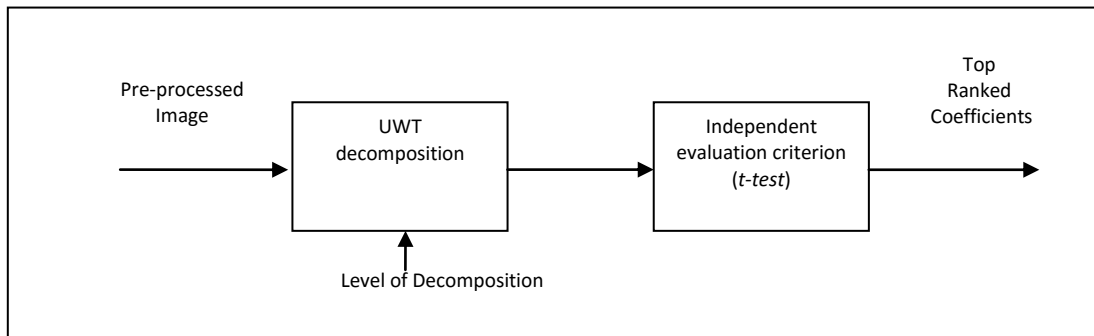


Fig 3: Proposed UWT based feature extraction stage for glaucoma detection

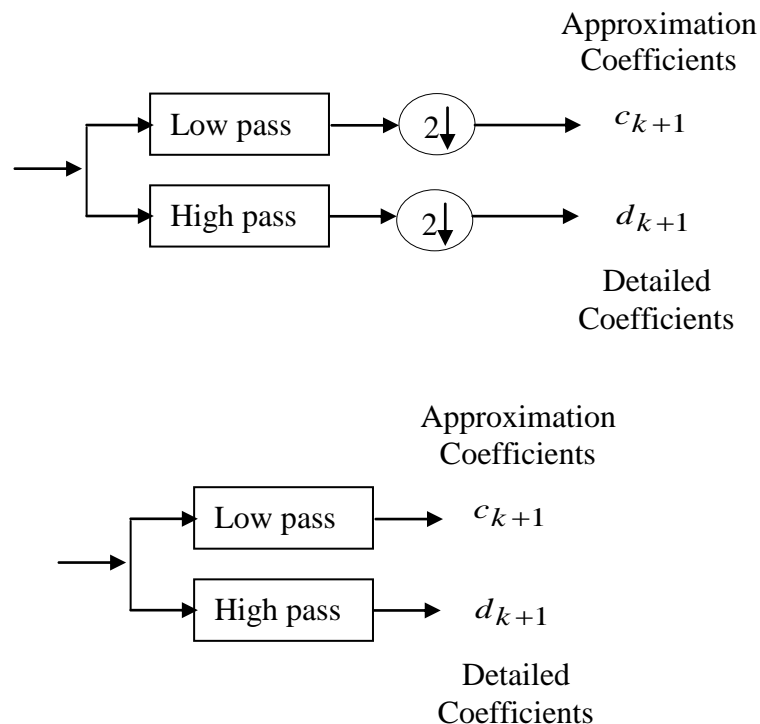


Fig 4: Decomposition filter design (a) DWT (b) UWT

As the down samplers are removed in the UWT filter design [14], there is no decimation take place. Hence, the size of the obtained sub-bands by UWT decomposition is same as the size of the input image. It produces a high dimensional feature space than the DWT feature space. Hence, an efficient feature selection algorithm is needed to reduce the dimensionality of the feature space. The proposed system uses the

independent evaluation criterion named *t-test* [15]. The procedure to find the top ranked coefficients is given below.

Let us consider the training samples of glaucomatous images (G) and non-glaucomatous images (NG), and then the *t-test* criterion is

$$t(x) = \frac{\text{mean}(G(x)) - \text{mean}(NG(x))}{\sqrt{\text{std}(G(x))/n_1 + \text{std}(NG(x))/n_2}} \quad (1)$$

where n_1 and n_2 is the number of training glaucomatous and non-glaucomatous images respectively. x is a particular feature position. Using eqn. 1, the t value is computed for features in the extracted feature space. It is known that the feature which has the highest t value is the best feature that discriminating the glaucomatous and non-glaucomatous images effectively.

Classification Stage

Glaucoma detection is employed in this stage which is also called validation stage. The features from the unknown OCT image are extracted using feature extraction stage explained in section 2.2. To train and test the proposed glaucoma detection system, SVM classifier is employed. Basically, SVM classifier is a binary classifier and it can be used for multiclass classification [16]. The proposed system is considered as a two class problem since the given OCT image is classified into either glaucomatous or non-glaucomatous images. Hence the proposed system requires a binary SVM classifier. The classification of OCT image is achieved by SVM using an optimal hyperplane as shown in Fig. 5 which separates the training features into glaucomatous (light coloured circle) or non-glaucomatous (dark coloured circle). The kernel functions; linear, quadratic, Radial Basis Function (RBF), polynomial, and Multilayer Perceptron (MLP) are employed in this study.

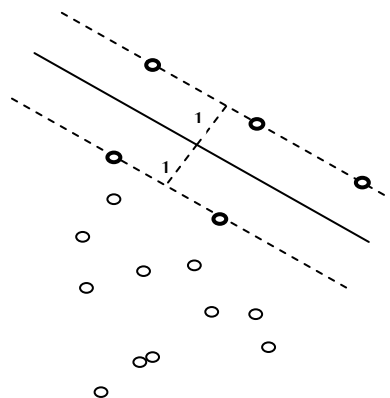


Fig 5: Optimal hyper plane constructed by SVM classifier

RESULTS AND DISCUSSIONS

The performances of the proposed glaucoma diagnosis system are discussed briefly in this section. A vast number of OCT images (100 normal OCT images and 100 glaucomatous OCT images) are used for the evaluation. All captured images are in RGB colour mode with 689x329 pixels resolution and saved in jpeg format. Many simulations are performed based on the UWT level of decomposition up to 6th level and number of top ranked coefficients (10% to 50% coefficients).

The proposed system is tested 10 times using randomly selected training and testing samples. In each simulation, the accuracy is computed as the ratio of the correctly classified OCT images to number of tested OCT samples. The classification accuracies tabulated in the following Tables 1 to 5 are the average classification accuracies from these 10 redundant simulation.

Table 1: Accuracies of the proposed system using 10% top ranked UWT coefficients

| UWT Level | SVM kernels (%) | | | | |
|-----------|-----------------|-----------|------------|-------|-------|
| | Linear | Quadratic | Polynomial | RBF | MLP |
| 1 | 68.32 | 80.23 | 62.62 | 63.44 | 59.64 |
| 2 | 68.79 | 65.45 | 59.19 | 64.21 | 62.85 |
| 3 | 69.37 | 61.82 | 62.16 | 66.64 | 62.16 |
| 4 | 71.71 | 63.14 | 65.37 | 68.84 | 60.74 |
| 5 | 69.78 | 61.27 | 61.81 | 67.36 | 64.19 |
| 6 | 60.90 | 55 | 60.45 | 62.88 | 51.36 |

Table 2: Accuracies of the proposed system using 20% top ranked UWT coefficients

| UWT Level | SVM kernels (%) | | | | |
|-----------|-----------------|-----------|------------|-------|-------|
| | Linear | Quadratic | Polynomial | RBF | MLP |
| 1 | 72.79 | 68.85 | 63.15 | 61.62 | 65.06 |
| 2 | 70.70 | 63.17 | 61.80 | 60.74 | 63.54 |
| 3 | 81.39 | 65.00 | 74.36 | 66.77 | 71.64 |
| 4 | 79.02 | 70.09 | 75.97 | 66.74 | 70.15 |
| 5 | 80.57 | 68.42 | 74.87 | 66.89 | 69.05 |
| 6 | 62.50 | 57.25 | 60.26 | 64.43 | 54.21 |

Table 3: Accuracies of the proposed system using 30% top ranked UWT coefficients

| UWT Level | SVM kernels (%) | | | | |
|-----------|-----------------|-----------|------------|-------|-------|
| | Linear | Quadratic | Polynomial | RBF | MLP |
| 1 | 79.19 | 72.88 | 72.32 | 58.22 | 70.01 |
| 2 | 77.10 | 70.68 | 72.65 | 58.71 | 72.12 |
| 3 | 84.84 | 70.78 | 77.32 | 61.36 | 71.56 |
| 4 | 80.74 | 74.66 | 79.29 | 61.97 | 69.31 |
| 5 | 81.20 | 70.70 | 77.92 | 59.08 | 64.42 |
| 6 | 64.22 | 59.65 | 65.25 | 60.25 | 56.68 |

Table 4: Accuracies of the proposed system using 40% top ranked UWT coefficients

| UWT Level | SVM kernels (%) | | | | |
|-----------|-----------------|-----------|------------|-------|-------|
| | Linear | Quadratic | Polynomial | RBF | MLP |
| 1 | 78.51 | 73.78 | 76.18 | 51.27 | 71.05 |
| 2 | 75.25 | 69.27 | 74.74 | 52.66 | 72.80 |
| 3 | 92.18 | 71.11 | 80.47 | 53.51 | 74.69 |
| 4 | 81.21 | 72.92 | 80.64 | 51.99 | 70.90 |
| 5 | 81.88 | 71.73 | 81.54 | 51.14 | 68.72 |
| 6 | 63.50 | 59.00 | 61.26 | 60.72 | 53.67 |

Table 5: Accuracies of the proposed system using 50% top ranked UWT coefficients

| UWT Level | SVM kernels (%) | | | | |
|-----------|-----------------|-----------|------------|-------|-------|
| | Linear | Quadratic | Polynomial | RBF | MLP |
| 1 | 76.96 | 75.22 | 77.41 | 50.30 | 74.76 |
| 2 | 75.42 | 71.18 | 77.16 | 50.30 | 73.90 |
| 3 | 84.39 | 71.57 | 81.70 | 50.60 | 77.22 |
| 4 | 78.80 | 69.85 | 79.51 | 50 | 71.21 |
| 5 | 81.43 | 72.91 | 83.31 | 50 | 71.39 |
| 6 | 64.01 | 60.68 | 65.39 | 55.58 | 55.17 |

It is observed from the simulation results in the Tables 1 to 5 that the maximum classification accuracy of the proposed system while using linear, quadratic, polynomial, RBF, and MLP kernel is 92.18%, 80.23%, 83.31%, 82.5% and 77.22% respectively. Also, it is noted that linear SVM produces better results for all the simulation tests than quadratic, polynomial, RBF, and MLP kernel. Further increase in the level of decomposition and more than 50% top ranked coefficients does not improve the accuracy due to the redundant data. To prove the efficacy of the proposed glaucoma detection system using UWT, the other techniques such as DWT [10] and PCA [8] are compared and their maximum classification accuracies are shown in Fig. 6 for five different kernels in SVM. It is observed from the Fig. 6 that the UWT features produce better results than DWT and PCA.

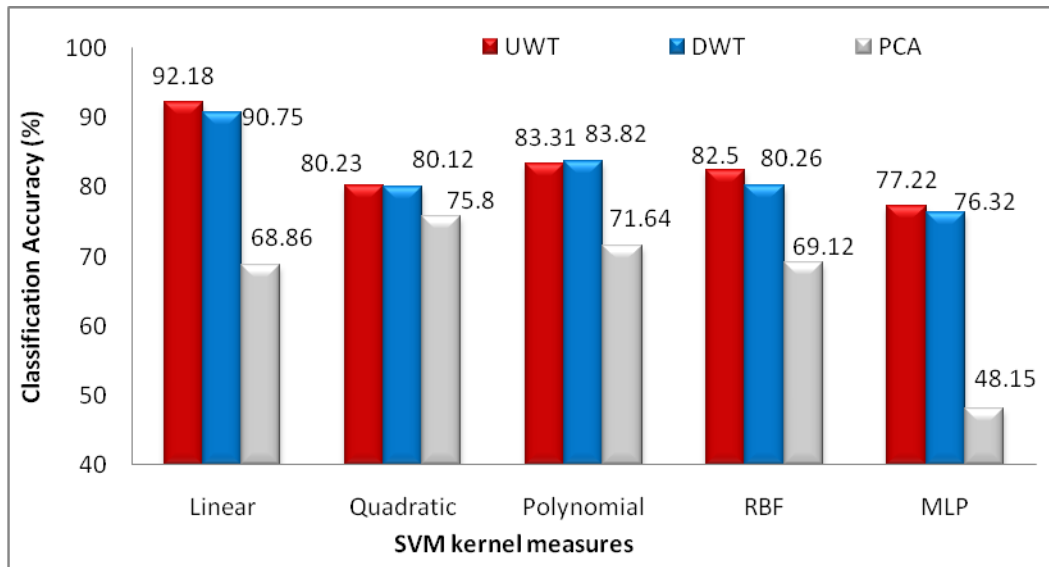


Fig 6: Comparative analysis of the proposed system with DWT and PCA

CONCLUSIONS

An efficient approach for the diagnosis of glaucoma using UWT and SVM classifier is presented in this paper. Before extracting UWT based features, the OCT images are pre-processed in order to remove the noise and then the retinal area is only cropped. From the high dimensional UWT feature space, the predominant features are selected using *t-test* approach. The selected features are tested using SVM classifier with various kernels. From the results, it is observed that linear SVM produces better result than other kernels with 92.18% accuracy. In future, sub-band fusion approach can be introduced before feature selection for better improvement.

REFERENCES

- [1] Artemas Herzog, KL, Boyer & Roberts, C, 'Extracting the optical disc endpoints in optical coherence tomography data', Proceedings of the 7th IEEE Workshops on Application of Computer Vision, 2005; 1: 263-268.
- [2] Boyer, K. L., Herzog, A., & Roberts, C., Automatic recovery of the optic nerve head geometry in optical coherence tomography. IEEE Transaction on Medical Imaging, 2006; 25(5): 553-570.
- [3] Gracitelli, C. P., Abe, R. Y., & Medeiros, F. A., Spectral-domain optical coherence tomography for glaucoma diagnosis. The open ophthalmology journal, 2015; 9: 68-77.
- [4] Ioannis Moupagiatzis, Mayer, M, Hornegger, J, Tornow, R & Mardin, C, 'Application of morphological operators for optic nerve head segmentation in optical coherence tomography images', 19th International Conference on Systems, Signals and Image Processing, 2012; 572-575.
- [5] Sumali Deb, Optical coherence tomography in nonglaucomatous optic nerve disorders. Ophthalmic Imaging, <http://www.oswb.org/journal/journal09/sumal.pdf>, 2009; 47-50. 30.

- [6] Ganesh Babu, T. R., Shenbaga Devi, S., & Venkatesh, R., Optic nerve head segmentation using fundus images and optical coherence tomography images for glaucoma detection. *Biomedical Papers*, 2015; 159(4): 607-615.
- [7] Ganeshbabu, T. R., Devi, S. S., & Venkatesh, R., Automatic Detection of Glaucoma Using Optical Coherence Tomography Image. *Journal of Applied Sciences.*, 2012; 12: 2128-2138.
- [8] Rajan, A & Ramesh, G. P, Glaucomatous Image Classification Based on PCA using Optical Coherence Tomography Images. *International Journal of Applied Engineering Research*, 2015; 10(17): 1-5.
- [9] Rajan, A., Ramesh, G. P., & Yuvaraj, Glaucomatous image Classification using Wavelet Transform. *IEEE International Conference on Advanced Communication Control and Computing Technologies*, 2014; 1398-1402.
- [10] Rajan, A., Ramesh, G. P., Automated Early Detection of Glaucoma in Wavelet Domain Using Optical Coherence Tomography Images. *Biosciences Biotechnology Research Asia*, 2015; 12(3): 2821-2828.
- [11] Rajan, A., Ramesh, G. P., Comparative Study of Glaucomatous Image Classification Using Optical Coherence Tomography. *International Journal of Pharmaceutical Sciences Review Research*, 2016; 36(1): 277-280.
- [12] Otsu, N., A Threshold Selection Method from Gray-Level Histograms, *IEEE Transactions on Systems, Man, and Cybernetics*. 1979; 9(1): 62-66.
- [13] S.G.Mallat, A theory for multi resolution signal Decomposition: The wavelet representation, *IEEE transactions on pattern analysis and machine intelligence.*, 1989; 11(7): 674-693.
- [14] Burrus, C. S., Gopinath, R. A., Guo, H., Odegard, J. E., andSelesnick, I. W., *Introduction to wavelets and wavelet transforms: a primer*, New Jersey: Prentice hall, 1998.
- [15] Wei Zhu, Xuena Wang, Yeming Ma, Manlong Rao, James Glimm, and John S. Kovach, Detection of cancer-specific markers amid massive mass spectral data, *Proceedings of the National Academy of Sciences*, 2003; 100(25):14666-14671.
- [16] Vapnik, V. N., *Statistical learning theory*, Wiley New York, 1998.